IMPERIAL COLLEGE of SCIENCE, TECHNOLOGY & MEDICINE

DEPARTMENT of ELECTRICAL & ELECTRONIC ENGINEERING

MSc in Communications and Signal Processing

Formal Report No. 2

(Please complete this form and attach it to the front of your report)

Name	Haoxiang Huang
Experiment Code	AM
Title of Experiment	Array Communications & Processing
Date of Submission	1/12/2024
Supervisor of Experiment	Prof. A. Manikas
Grade	

Communications, Control and Signal Processing Laboratory

Array Communications and Processing

* Submission for M.Sc. C&SP 2nd Formal Lab Report at Imperial College London

Haoxiang Huang
Department of Electrical and Electronic Engineering
Imperial College London
SW7 2AZ, London, U.K.
haoxiang.huang23@imperial.ac.uk

***Abstract*—This experiment investigates an array receiver framework for SIMO and MIMO, employing differential geometry to integrate space-time information in array processing. This theoretical framework emphasizes the "superresolution" approach to address three key problems: detection, estimation, and reception. This framework enhances handling of complex signals for SIMO and MIMO, contributing significantly to the advancement of array communication systems.**

***Index Terms*—Array Communications, Differential Geometry in Array Processing, Array Receiver Framwork, SIMO, MIMO, MuSIC Algorithm, Superresolution Beamformer, Wiener-Hopf Beamformer, AIC Criterion and MDL Criterion.**

I. Introduction

THE advance of digital communication systems has seen a paradigm shift towards sophisticated array signal processing technologies, notably the development of differential geometry in array communication and signal processing [1]. This experiment focuses on such arrays, formed by distributing numerous receiving elements, referred to as sensors, in a 3-dimensional Cartesian space. The area over which these sensors are distributed is known as the aperture of the array. The primary challenge in array processing is to extract information about a signal environment, consisting of various emitting sources plus noise, from the waveforms received at these array elements.

In fields like radar-based systems, these emitting sources often represent targets that either reflect transmitted signals (active radars) or emit their own signals (passive radars). The application of arrays extends beyond radar systems to radio telescopy, sonar and to geophysics etc. However, a particularly 'hot' application area is digital communications, where array theory is integrated with differential geometry theory to exploit space-time information. This integration leads to new communication system architectures that considerably enhance the capacity and performance of mobile communication networks. These improvements manifest in various forms, such as suppressing co-channel interferences, combating fading effects, and accurately locating or tracing mobile users [2].

This experiment presents a theoretical array receiver framework for SIMO and MIMO that applied differential geometry in array communication to addresses various problems in these diverse applications. Emphasis will be placed on "superresolution" approaches to tackle three general problems: detection, estimation, and reception. We address the detection problem in array signal processing with a focus on identifying the number of cochannel emitting sources. We consider two scenarios: one where infinite observation snapshots of received signals are available, and the number of sources is estimated directly from the eigenvalues of the signal covariance matrix; and a second scenario with finite snapshots, where the Akaike Information Criterion (AIC) or Minimum Description Length (MDL) criteria are employed [2] [3]. For estimating the DOAs, our experiment emphasises a superresolution approach using the MuSIC algorithm. This method is particularly effective for accurately determining the sources' directions compared to traditional Fourier methods [2] [4]. Additionally, we introduced an advanced pre-processor called the 'spatial-smoothing' technique, which effectively correct the coherent signal problem. In the reception problem, we investigate a superresolution beamformer [5], designed to effectively receive the desired signal while eliminating co-channel interferences at low SNR level. Additionally, we also conduct a comparative analysis between this superresolution beamformer and the conventional Wiener-Hopf Beamformer.

Thus, this experiment not only provides a comprehensive examination of the aforementioned concepts but also gives a comparison with other traditional methods on array processing. This proposed array receiver architecture for SIMO and MIMO in this experiment leads to a comprehensive approach to effectively handle these three receiver challenges and significantly contributes to the advancement of array communication systems.

II. Background

A. Array of Sensor - Environment

An array is formed by distributing a number N of sensors (such as transducing elements, antennas, or receivers) in a 3-dimensional Cartesian space, all sharing a common reference point. The sensor positions are defined by the matrix $\mathbf{r} \in \mathbb{R}^{3\times N}$

$$\mathbf{r} = \begin{bmatrix}\mathbf{r}_1 & \mathbf{r}_2 & \dots & \mathbf{r}_N\end{bmatrix} = \begin{bmatrix}\mathbf{r}_x \\ \mathbf{r}_y \\ \mathbf{r}_z\end{bmatrix} \tag{1}$$

where $\mathbf{r}_k = [x_k, y_k, z_k]^T$ represents the Cartesian coordinates (location) of the k-th sensor in the array, for $k = 1, 2, \dots, N$.

The direction of a wave impinging on the array is typically described using two angles: the azimuth angle θ, measured counterclockwise from the positive x-axis, and the elevation angle ϕ, measured counterclockwise from the x-y plane (as shown in Fig. 1).

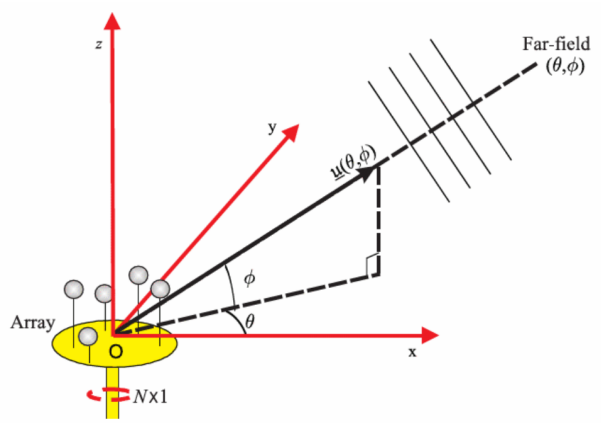

Fig. 1: Relative geometry between a far-field emitting source and an array of sensors [1].

Correspondingly, the direction is represented by a 3×1 real unit-norm vector.$\mathbf{u}(\theta, \phi)$:

$$\mathbf{u}(\theta, \phi) = \begin{bmatrix} \cos\theta \cos\phi \\ \sin\theta \cos\phi \\ \sin\phi \end{bmatrix} \tag{2}$$

and

$$\|\mathbf{u}(\theta, \phi)\| = 1 \tag{3}$$

Then, the wavenumber vector $\mathbf{k}(\theta, \phi)$ is defined as following:

$$\mathbf{k}(\theta, \phi) = \frac{2\pi}{\lambda} \cdot \mathbf{u}(\theta, \phi) \tag{4}$$

In this experiment, we consider the standard Uniform Linear Array (ULA) with 5 sensors are uniformly distributed at one halfwavelength along the x-axis. The coordinates of this ULA in 3-dimensional Cartesian space is given as following:

$$\mathbf{r} = \begin{bmatrix} -2 & -1 & 0 & 1 & 2 \\ 0 & 0 & 0 & 0 & 0 \\ 0 & 0 & 0 & 0 & 0 \end{bmatrix} \tag{5}$$

B. Array Manifold Vector

Array signal processing for signal sources detection, channel estimation, beamforming, etc., can be more effective with the properties and parameters of the array manifold [6]. The manifold of an array consisting of N sensors is conceptualized from differential geometry as a surface within an N-dimensional complex space, defined as a function of azimuth and elevation angles [7]. Considering the $(N \times 1)$ complex vector $\mathbf{S}$, i.e., $\mathbf{S} \in \mathbb{C}^{N \times 1}$, is defined as

$$\mathbf{S}(\theta, \phi) = \exp(-j[\mathbf{r}_1, \mathbf{r}_2, \ldots, \mathbf{r}_N]^T \mathbf{k}(\theta, \phi)) \tag{6}$$

where $\mathbf{S}(\theta, \phi)$ is known as the array manifold vector and represents the response of the array for an electromagnetic signal of unity power (i.e., $\|\mathbf{E}(0, 3, t)\|^2 = 1$) and direction of propagation (θ, ϕ), and $\mathbf{k}(\theta, \phi)$ is the wavenumber vector [3].

C. Multi-path SIMO Channel Modeling

The impulse response (vector) of the SIMO multipath channel is shown in Fig. 2 and defined as following:

$$h(t) = \sum_{\ell=1}^{L} S(\theta_\ell, \phi_\ell) \cdot \beta_\ell \cdot \delta(t - \tau_\ell) \tag{7}$$

where L means the the number of paths and (θ_ℓ, ϕ_ℓ) denotes the DOA from which the ℓ-th path reaches the reference point of the antenna array. Additionally, β_ℓ, τ_ℓ represent the channel fading coefficient and the delay associated with the ℓ-th path, respectively.

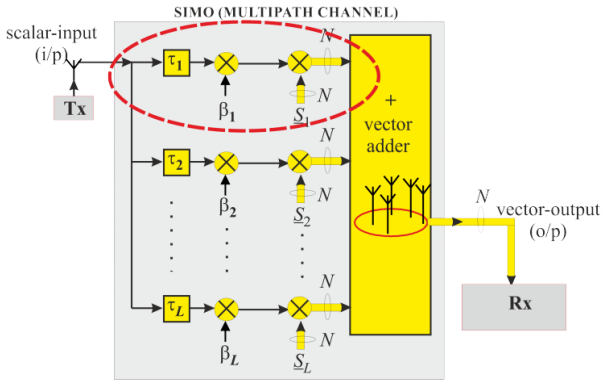

Fig. 2: Wireless SIMO Channel Modelling [3].

The received $(N \times 1)$ vector-signal $\mathbf{x}(t)$ through this SIMO channel can be modeled as follows:

$$\mathbf{x}(t) = \mathbf{h}(t) \cdot \mathbf{m}(t) + \mathbf{n}(t) \tag{8}$$

$$= \sum_{\ell=1}^{L} \mathbf{S}(\theta_\ell, \phi_\ell) \cdot \beta_\ell \cdot \delta(t - \tau_\ell) \cdot \mathbf{m}(t) + \mathbf{n}(t) \tag{9}$$

$$\mathbf{x}(t) = \sum_{\ell=1}^{L} \mathbf{S}(\theta_\ell, \phi_\ell) \cdot \beta_\ell \cdot \mathbf{m}(t - \tau_\ell) + \mathbf{n}(t) \tag{10}$$

$$= \mathbf{S}\mathbf{m}(t) + \mathbf{n}(t) \tag{11}$$

where

$$\mathbf{S} = [\mathbf{S}_1, \mathbf{S}_2, \ldots, \mathbf{S}_L], \quad \text{with } \mathbf{S}_\ell \triangleq \mathbf{S}(\theta_\ell, \phi_\ell) \tag{12}$$

$$\mathbf{m}(t) = [\beta_1 \mathbf{m}(t - \tau_1), \beta_2 \mathbf{m}(t - \tau_2), \ldots, \beta_L \mathbf{m}(t - \tau_L)]^T \tag{13}$$

and $\mathbf{n}(t)$ is the additive white noise (AWGN).

Next, consider a receiver (Rx) array with N antennas operating in the presence of M co-channel transmitters/users. To distinguish between the transmitters, a subscript i is used, referring to the i-th transmitter. The received $(N \times 1)$ vector-signal $\mathbf{x}(t)$ from all M transmitters/users (which transmit simultaneously on the same frequency band) can be modeled as follows [3]:

$$\mathbf{x}(t) = \sum_{i=1}^{M} \sum_{\ell=1}^{L} \mathbf{S}_{i\ell} \cdot \beta_{i\ell} \cdot \mathbf{m}_i(t - \tau_\ell) + \mathbf{n}(t) \tag{14}$$

where $\mathbf{S}_{i\ell} = \mathbf{S}(\theta_{i\ell}, \phi_{i\ell})$.

D. Array Pattern

The array receives data plus noise from three transmitters operating at same frequency bands. The DOA of these sources in this experiment is: (30°,0°), (35°,0°), and (90°,0°). In these coordinates, the first value indicates the azimuth angles while the second denotes the elevation angles. The pattern of the array can be used to assess the array's gain across different directions, and this is defined by:

$$g(\theta, \phi) = \mathbf{w}^H \mathbf{S}(\theta, \phi) \tag{15}$$

where $\mathbf{w}^H$ denotes the complex weights and $\mathbf{S}(\theta, \phi)$ represents the array manifold vectors.

When $\mathbf{w} = \underline{1}_N$, the function $g(\theta, \phi)$ describes the antenna array's default pattern without beamformer. In this experiment, the default array pattern is shown as Fig. 3

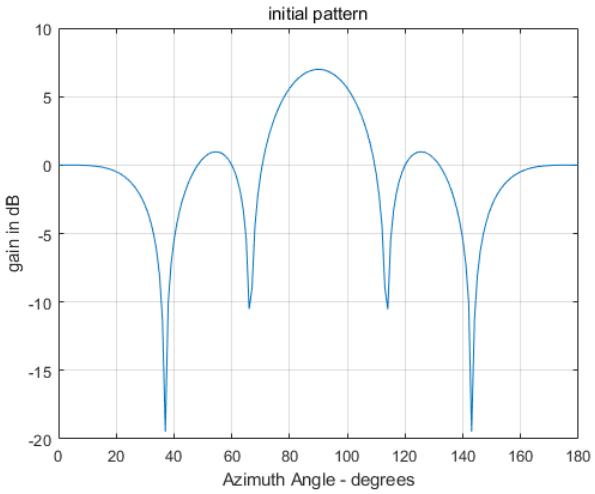

Fig. 3: The Initial Array Pattern

E. Array Covariance Matrix

1) Theoretical Covariance Matrix: If the received $(N \times 1)$ vector-signal $\mathbf{x}(t) = \mathbf{S}\mathbf{m}(t) + \mathbf{n}(t)$ can be observed over an infinite interval. This allows for the calculation of its second-order statistics. Thus, the theoretical covariance matrix $\mathbf{R}_{xx}$ is given by

$$\mathbf{R}_{xx} = \mathbb{E}\left\{\mathbf{x}(t)\mathbf{x}^H(t)\right\} \tag{16}$$

$$= \mathbf{S}\mathbf{R}_{mm}\mathbf{S}^H + \mathbf{R}_{nn} \tag{17}$$

where, $\mathbf{S}$ is the array manifold vectors, $\mathbf{R}_{mm}$ and $\mathbf{R}_{nn}$ is the covariance matrix of the sources and covariance matrix of noise. In this experiment, noise is AWGN and $R_{nn} = \sigma^2\mathbf{I}$.

2) Practical Covariance Matrix: In practice, we can only observe over finite observation interval equivalent to L snapshots. Thus, the 2nd order statistics of x(t) are estimated as following:

$$\mathbf{R}_{xx} = \frac{1}{L}\sum_{l=1}^{L} \mathbf{x}(t_l)\mathbf{x}^H(t_l) \tag{18}$$

where t_l is the sampled at time t_l of the snapshot.

III. Array Receivers Framework for SIMO and MIMO

In the context of array receivers, our primary goal is to derive meaningful insights from a vector received signal $x(t) = S_m(t) + n(t)$, reflecting the complexity of signal environments. In this experiment, we proposed the array receivers framework for SIMO and MIMO (shown as Fig. 4) to tackling three general problems for a receiver.

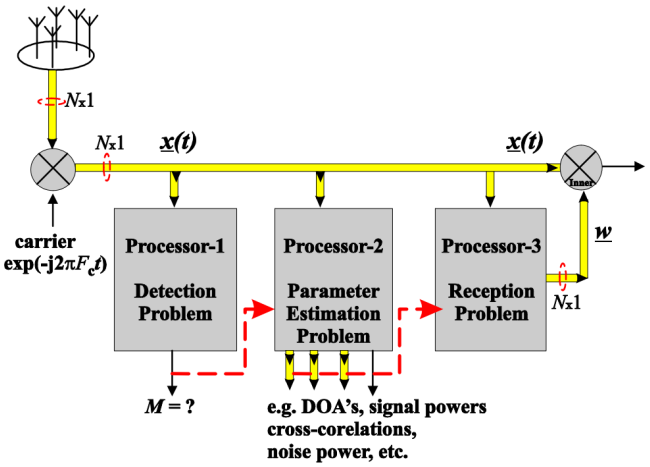

Fig. 4: Array Receivers Framework for SIMO and MIMO [3]

First, the Detection Problem is focused on identifying the number of co-channel sources, symbolized as M. This determines the presence of multiple signal sources.

Second, the Estimation Problem requires computing a range of signal and channel parameters. This includes the Directions of Arrival (DOAs) θ_i using MuSIC algorithm. It also involves some factors such as polarization parameters, fading coefficients, and signal spread etcs [3].

Lastly, the Reception Problem is to construct a weight vector which is going to isolate a "desired" signal in space while efficiently suppressing interference from the other $M-1$ signals using beamformer such as WIENER-HOPF Beamformer and Superresolution Beamformer.

IV. Detection Problem

A. Theoretical Approach

By applying eigen-decomposition to R_x in Equation (17), we obtain:

$$\mathbf{R}_{xx} = \mathbf{E} \cdot \boldsymbol{D} \cdot \mathbf{E}^H \tag{19}$$

$$= \mathbf{E} \cdot \boldsymbol{\Sigma} \cdot \mathbf{E}^H + \sigma^2\mathbf{I}_N \tag{20}$$

$$= \mathbf{E} \cdot (\boldsymbol{\Sigma} + \sigma^2\mathbf{I}_N) \cdot \mathbf{E}^H \tag{21}$$

where $\mathbf{\Sigma}$ is an $N \times N$ diagonal eigenvalues matrix of the $\mathbf{R}_{mm}$, and it is:

$$\mathbf{\Sigma} = \begin{bmatrix} \lambda_1 & 0 & \cdots & 0 & 0 & \cdots & 0 \\ 0 & \lambda_2 & \cdots & 0 & 0 & \cdots & 0 \\ \vdots & \vdots & \ddots & \vdots & \vdots & \ddots & \vdots \\ 0 & 0 & \cdots & \lambda_M & 0 & \cdots & 0 \\ 0 & 0 & \cdots & 0 & 0 & \cdots & 0 \\ \vdots & \vdots & \ddots & \vdots & \vdots & \ddots & \vdots \\ 0 & 0 & \cdots & 0 & 0 & \cdots & 0 \end{bmatrix} \tag{22}$$

Thus, eigenvalues matrix $\boldsymbol{D}$ of the $\mathbf{R}_{xx}$ is:

$$\begin{aligned} \mathbf{D} &= \mathbf{\Sigma} + \sigma^2 \mathbf{I}_N \qquad (23) \\ &= \begin{bmatrix} \lambda_1 + \sigma^2 & 0 & \cdots & 0 & 0 & \cdots & 0 \\ 0 & \lambda_2 + \sigma^2 & \cdots & 0 & 0 & \cdots & 0 \\ \vdots & \vdots & \ddots & \vdots & \vdots & \ddots & \vdots \\ 0 & 0 & \cdots & \lambda_M + \sigma^2 & 0 & \cdots & 0 \\ 0 & 0 & \cdots & 0 & \sigma^2 & \cdots & 0 \\ \vdots & \vdots & \ddots & \vdots & \vdots & \ddots & \vdots \\ 0 & 0 & \cdots & 0 & 0 & \cdots & \sigma^2 \end{bmatrix} \end{aligned}$$

Remark 1. *Theoretically, if $L = \infty$, i.e., Theoretical $\mathbf{R}_{xx} = \mathbb{E}\left[\mathbf{x}(t)\mathbf{x}^H(t)\right]$, then the number of emitting source M and noise power σ_n^2 can be determined by the eigenvalues of the covariance matrix Rxx of the Rx signal-vector x(t), and more specifically by the following expression [3]:*

$$M = N - \textit{(multiplicity of min eigenvalue of } \mathbf{R}_{xx}\textit{)} \tag{24}$$

$$\sigma_n^2 = \textit{min eigenvalue of } \mathbf{R}_{xx} = \textit{noise power} \tag{25}$$

In Matlab simulation of this experiment, we set $\sigma_n^2 = 0.0001$, the theoretical eigenvalue matrix of the R_{xx} is

$$\mathbf{R}_{xx,theoretical} = \begin{bmatrix} 9.9369 \\ 4.9681 \\ 0.0953 \\ 0.0001 \\ 0.0001 \end{bmatrix}, \tag{26}$$

Based on the Remark 1, We can easily find the the multiplicity of minimum eigenvalues is 2 and last two same eigenvalues is the noise power σ^2. Thus, the estimated number of emitting sources $M = N - 2 = 5 - 2 = 3$.

B. Practical Approach

However, in practice:

$$\sigma_1^2 \neq \sigma_2^2 \neq \ldots \neq \sigma_M^2 \neq \sigma_{M+1}^2 \neq \ldots \neq \sigma^2, \tag{27}$$

This means that the theoretical approach always fails to accurately estimate the multiplicity of minimum eigenvalue. This also can be validated by the real audio and image signals given in our experiment. According to Equation (14), the eigenvalues matrix of $\mathbf{R}_{xx,audio}$ and $\mathbf{R}_{xx,image}$ are estimated below:

$$\mathbf{Eig}_{xx,audio} = \begin{bmatrix} 4.3818 \times 10^5 \\ 1.072 \times 10^4 \\ 1.733 \times 10^2 \\ 0.0101 \\ 0.0100 \end{bmatrix} \tag{28}$$

$$\mathbf{Eig}_{xx,image} = \begin{bmatrix} 2.178 \times 10^5 \\ 2.039 \times 10^4 \\ 190.87 \\ 7.0614 \times 10^{-11} \\ -9.4922 \times 10^{-11} \end{bmatrix} \tag{29}$$

Obviously, $\sigma_4^2 \approx \sigma_5^2$, but they are not exactly equal. In this case, more powerful the information theoretic criterias [8] including the Akaike Information Criterion (AIC) and Minimum Description Length (MDL) criteria are introduced in the practice. The AIC and MDL is defined as following:

$$\begin{aligned} \text{AIC}(k) = &- 2\ln\left(\frac{\prod_{\ell=k+1}^{N} d_\ell^{\frac{1}{N-k}}}{\frac{1}{N-k}\sum_{\ell=k+1}^{N} d_\ell}\right)^{(N-k)L} \\ &+ 2k(2N-k) \end{aligned} \tag{30}$$

$$\begin{aligned} \text{MDL}(k) = &- \ln\left(\frac{\prod_{\ell=k+1}^{N} d_\ell^{\frac{1}{N-k}}}{\frac{1}{N-k}\sum_{\ell=k+1}^{N} d_\ell}\right)^{(N-k)L} \\ &+ \frac{1}{2}k(2N-k)\ln(L) \end{aligned} \tag{31}$$

where $k \in \{0, 1, \ldots, N-1\}$ and d_l is the l-th eigenvalue of Rxx.

Remark 2. *If L is finite, i.e., the practical R_{xx} is given as Equation (18). Here, M, the estimated number of sources, can be determined using the AIC or MDL criteria as specified in Equation (30) and Equation (31). Furthermore, the noise power σ_n^2 is the average of the $N - M$ smallest eigenvalues, denoted by [3]*

$$\sigma_n^2 = \frac{1}{N-M}\sum_{i=M+1}^{N} \sigma_i^2. \tag{32}$$

In our experiment, we simulate 250 snapshots with $\sigma_n^2 = 0.0001$, and compute the covariance matrix $\mathbf{R}_{xx}$ based on the Equation (18).The eigenvalues of this $\mathbf{R}_{xx}$ are:

$$\mathbf{Eig}_{xx,snapshots} = \begin{bmatrix} 9.22 \\ 5.17 \\ 0.087 \\ 1.024 \times 10^{-4} \\ 8.855 \times 10^{-5} \end{bmatrix} \tag{33}$$

Obviously $\sigma_4^2 \approx \sigma_5^2$, but they are not exactly equal as well. This means theoretical estimation approach fails in this case.

According to the Equation (30) and Equation (31), each values of $AIC(k)$ and $MDL(K)$ can be obtained as shown in the TABLE I.

TABLE I: AIC and MDL Values

k	0	1	2	3	4
AIC (k)	1120.4	1022.2	520.84	44.628	48.0
MDL (k)	560.2	512.66	263.24	59.29	66.3
Minimum	M = 3				

In Table I, the columns highlighted in green denote the minimum values of both AIC and MDL. Consequently, the estimated number of emitting sources, $M = 3$, corresponds to the indices of these minimum values. This indicates that the AIC and MDL criteria are robust against variations in noise power when estimating the number of emitting sources in practical scenarios.

V. Estimation Problem

Following the detection of the number of sources M, the subsequent challenge for the array receivers is the estimation problem. This problem aims to estimate signal and channel parameters includes determining the Directions of Arrival (DOAs), Time of Arrivals (TOAs), fading coefficients, and other relevant metrics. In our experiment, we estimate DOAs under two distinct scenarios: the uncorrelated sources and the coherent sources.

A. The uncorrelated sources

First, we consider the case where sources from (30°,0°), (35°,0°) and (90°,0°), and covariance matrix of $\mathbf{R}_{mm}$ is uncorrelated, represented as follows:

$$\mathbf{R}_{mm} = \begin{bmatrix} 1 & 0 & 0 \\ 0 & 1 & 0 \\ 0 & 0 & 1 \end{bmatrix} \tag{34}$$

Here, a signal subspace method called MuSIC algorithm [9] is used. The main idea of this algorithm is to find the intersection of the manifold with the signal subspace $\mathbf{L}[E_s]$, which provide the estimated parameters. Due to the orthogonality between the signal subspace and the noise subspace, The cost function is defined based on the projection of the manifold onto the noise subspace. This Cost function aids in finding the intersection as defined below:

$$\xi(\mathbf{p}) = \frac{1}{\underline{\mathbf{S}}(\mathbf{p})^H \cdot \mathbf{P}_{\mathbf{E}_n} \cdot \underline{\mathbf{S}}(\mathbf{p})} \tag{35}$$

where $\underline{\mathbf{S}}$ is the the array manifold vector, p is estimated parameters, and $\mathbf{P}_{\mathbf{E}_n}$ is the projection onto the noise subspace.

Based on the R_{mm} defined as Equation (34), the MuSIC spectrum of cost function $\xi(\mathbf{p})$ is shown as Fig.5. Here, the three peak points is the estimated DOA (30°,35°,90°), which is same as the ground-truth.

For the real audio and image signals given in our experiment, they can also be used to generate a similar MuSIC spectrum shown as Fig. 6 and Fig. 7. They also obtain the same estimated DOAs as mentioned above.

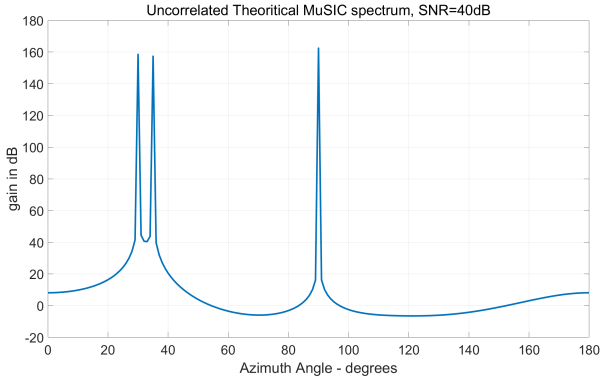

Fig. 5: Uncorrelated Theoritical MuSIC spectrum

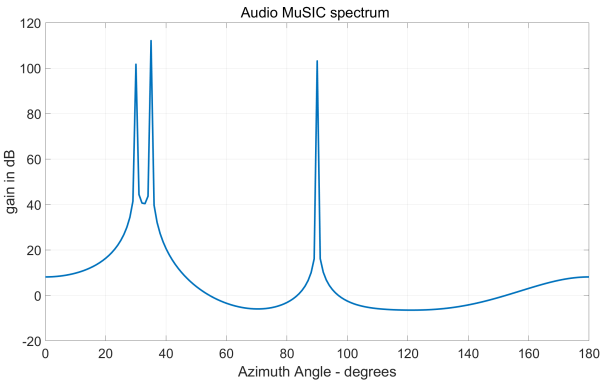

Fig. 6: Audio MuSIC spectrum

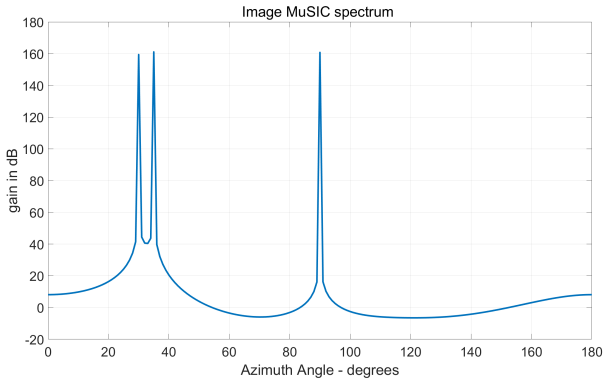

Fig. 7: Image MuSIC spectrum

B. The coherent sources

Alternatively, our experiment also examine a situation where two sources, specifically in the directions of (30°,0°) and (35°,0°), are fully correlated. In this case, $\mathbf{R}_{mm}$ is characterized by:

$$\mathbf{R}_{mm} = \begin{bmatrix} 1 & 1 & 0 \\ 1 & 1 & 0 \\ 0 & 0 & 1 \end{bmatrix} \tag{36}$$

Appling MuSIC algorithm in V-A to this theoritical signals, the obtained MuSIC spectrum of cost function $\xi(\mathbf{p})$ is shown

as Fig.8. Obviously, there are only two peaks at (90°, 0°) and (33°, 0°), while the fully correlated directions of (30°, 0°) and (35°, 0°) cannot be successfully identified.

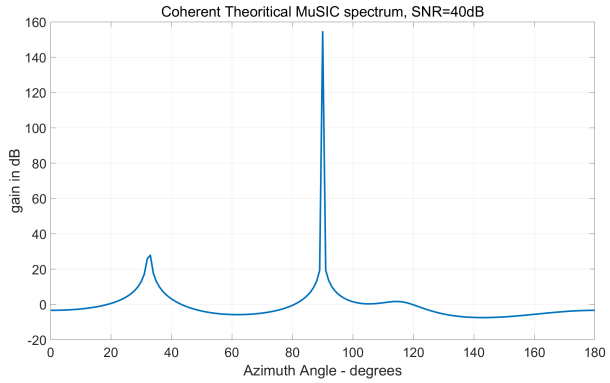

Fig. 8: Coherent Theoritical MuSIC spectrum

In this cases, a pre-processer is used before the MuSIC algorithm to "correct", which is known as the "spatial smoothing" [4]. The fundamental concept of 'spatial smoothing' involves computing average of all the partitioned sub-array to form the smoothed covariance matrix $R_{xx,smoothing}$, which then replaces the original covariance matrix in the MuSIC algorithm. The smoothed covariance matrix is defined as below:

$$R_{xx,smoothing} = \frac{1}{N}\sum_{s=1}^{N} R_s \tag{37}$$

Where $R_s(K \times K)$ is the partitioned sub-array with deterministic length K.

Based on the R_{mm} defined as Equation (34), the MuSIC spectrum of cost function $\xi(\mathbf{p})$ after "spatial smoothing" is shown as Fig.9. Here, the three peak points is correctly to be estimated as the DOA (30°,35°,90°), which is same as the ground-truth.

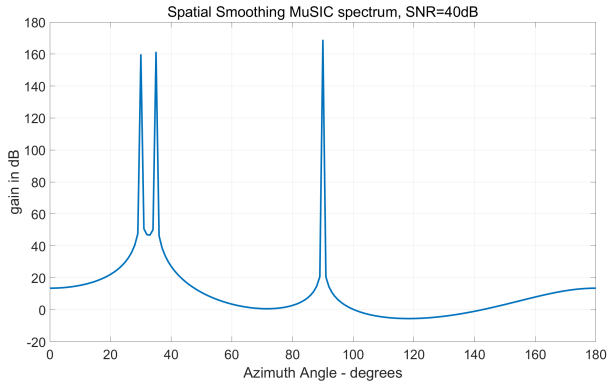

Fig. 9: Spatial Smoothing MuSIC spectrum

VI. Reception Problem

For the reception problem, it's important to construct a weight vector that isolates a 'desired' signal in space while suppressing all other 'unwanted' signals. Beamforming, a widely used technique, synthesizes an array pattern that achieves high gain in the direction of the desired signal's DOA while creating deep nulls towards the DOAs of interfering signals, effectively addressing the reception problem.

In our experiment, we will focus primarily on the more powerful 'Superresolution' Beamformer, and conduct a comparative analysis with the 'Wiener-Hopf' Beamformer and some Adaptive Beamformers (see Appendix for details).

A. Wiener-Hopf Beamformer

The weight of the Wiener-Hopf beamformer is defined as:

$$\underline{\mathbf{w}} = c \cdot \mathbf{R}_{xx}^{-1}\underline{\mathbf{S}}_d \tag{38}$$

where c is a constant scalar and $\underline{\mathbf{S}}_d$ is array manifold vector of desired signal [3].

Referring to R_{mm} as defined in Equation (34), and assuming that the desired source is positioned at (90°, 0°), the array pattern of the theoretical signal corresponding to $10dB$ and $40dB$ is illustrated as Fig. 10 and Fig. 11:

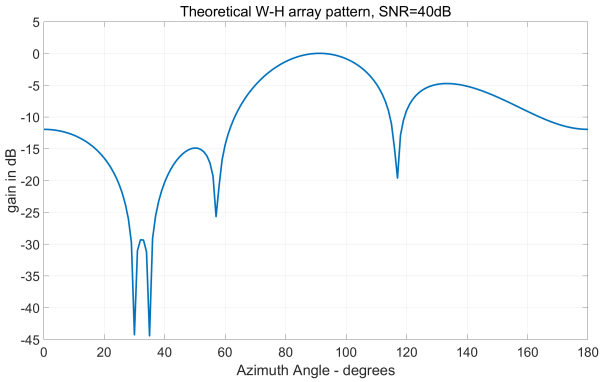

Fig. 10: Theoretical W-H array pattern, SNR= 40 dB

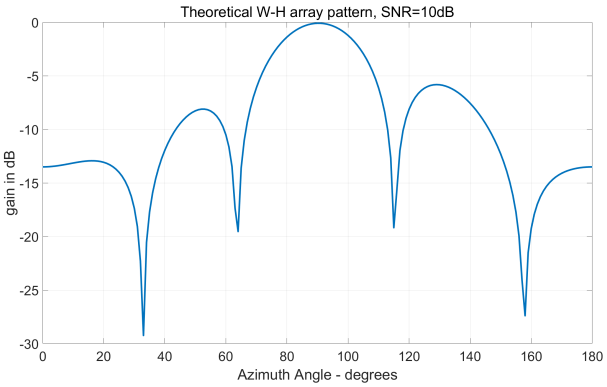

Fig. 11: Theoretical W-H array pattern, SNR= 10 dB

We can find that when the SNR is low, such as at 10 dB, nulls may not form at the two unknown interference DOAs (30°, 35°). Nonetheless, the system maintains optimal SNIR performance. when the SNR is high, it can perform well on SNIR and suppress all interference DOAs.

Remark 3. *The Wiener-Hopf (W-H) beamformer allows a degree of interference to reach the output, aiming to diminish strong noise and, in turn, maximize SNIR. Consequently, the performance of the W-H beamformer is the function of SNIR/SNR. High SNR levels lead to the formation of nulls at all DOAs of interference in the array pattern, which does not occur when the SNR is low.*

The SNR-sensitive property of W-H beamformer may lead to fail in some cases, which can also validate in our experiment. Here, the W-H beamformer is used to recieve the real audio and image signal after detection and estimation phases.

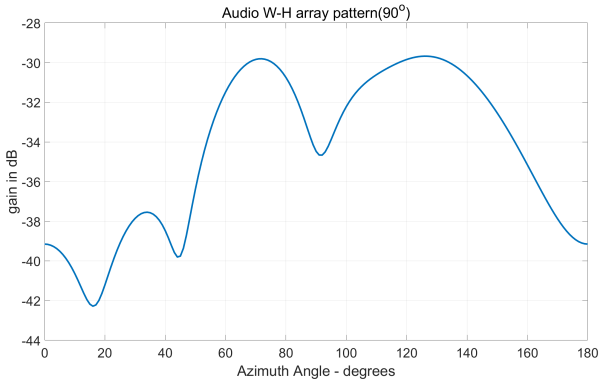

Fig. 12: Audio W-H Beamformer array pattern

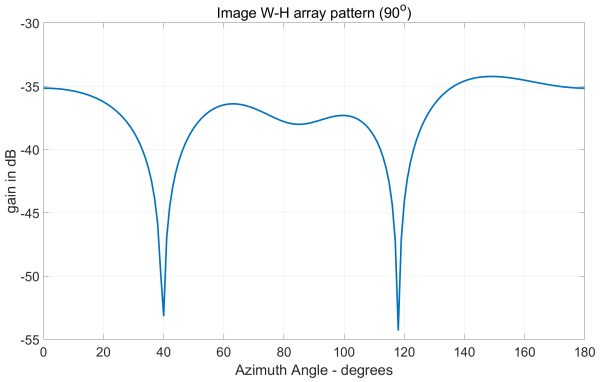

Fig. 13: Image W-H Beamformer array pattern

Fig. 14: The received image of W-H beamformer (90^o)

The array pattern of the receiver illustrated as Fig. 12 , Fig. 13 indicates the W-H beamformer fails to suppress the interfence DOAs. Additionally, the received image of W-H beamformer with 90^o DOA also aliases with some inference illustrated as Fig. 14

B. Superresolution Beamformer

A Superresolution Beamformer is not based on DOA estimation of interfering sources and defined as following [3]:

$$\mathbf{w} = \mathbf{P}_{\mathbf{E}_{\text{nj}}}\, \mathbf{S}_{\text{desired signal}} \tag{39}$$

Similarly, the superresolution beamformer is used to recieve the real image signal after detection and estimation phases. The array pattern and received image are illustrated as Fig. 15. These demonstrate that the superresolution beamformer effectively suppresses interference signals even at low SNR levels.

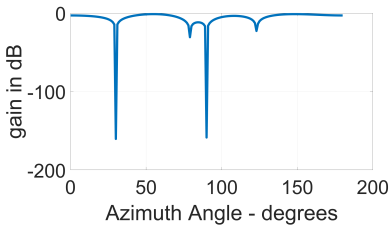

(a) Array Pattern, 35^o

(b) Received Image, 35^o

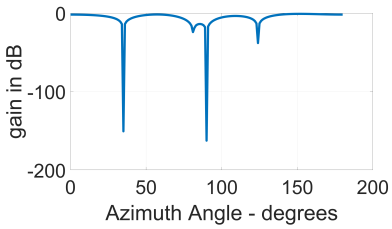

(c) Array Pattern, 30^o

(d) Received Image, 30^o

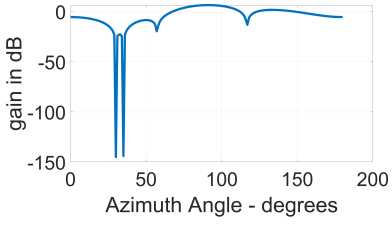

(e) Array Pattern, 90^o

(f) Received Image, 90^o

Fig. 15: Superresolution Beamformer array pattern and received image

VII. CONCLUSION

In this experiment, we implement a array receiver framework integrated with differential geometry for SIMO and MIMO systems, significantly advancing array communications. Our focus was on addressing three general receiver problems: detection, estimation, and reception. We employed the Akaike Information Criterion (AIC) or Minimum Description

Length (MDL) for efficient source number detection in practical finite snapshot scenarios. The MuSIC algorithm, under our superresolution approach, proved superior in estimating Directions of Arrival (DOAs), essential for various applications. Additionally, we introduced an advanced pre-processor called the 'spatial-smoothing' technique, which effectively countered coherent signal. our superresolution beamformer demonstrated remarkable efficacy in signal reception and interference suppression, especially in low SNR environments, compared to conventional W-H beamformers. This framework marks a significant contribution to the array communication systems.

APPENDIX: ADAPTIVE BEAMFORMER

The W-H Beamformer and Superresolution Beamformer highly depend on the second order statistics. However, these statistics are often unknown. By assuming ergodicity, it is possible to estimate these statistics, and consequently the optimal weights, from the data at hand. However, in mobile communication systems, the spatial position of the user and these statistics may change frequently. This requires real-time updates of the beamforming weight vector according to the user's current location. To address these challenges, the Adaptive Beamformer algorithms are commonly employed to determine the appropriate weights [11]. The general adaptive array systems illustrated as Fig. 16 that can dynamically adjust radiation in user's direction in response to the varying environment of the signal [12]. Thus, we also further investigate the Adaptive Beamformer as a supplementary beamformer for the array reception problem.

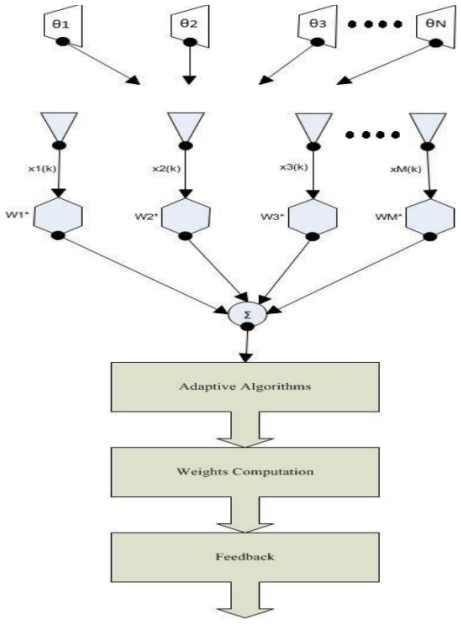

Fig. 16: Block diagram for adaptive beamforming [12]

A. LMS

The Least Mean Squares (LMS) algorithm is a simple and effective adaptive beamformer used to minimize mean error in signal processing. The SD approximation in terms of weights iteration using LMS method mathematically written as [12]:

$$e(k) = d(k) - w^H(k)x(k) \tag{40}$$

$$w(k+1) = w(k) + \mu e^*(k)x(k) \tag{41}$$

Where, $d(k)$ is the reference signal, $x(k)$ is the received signal vector, $w(k)$ is the weight vector, $e(k)$ is the error vector, and μ is the step size.

B. RLS

The Recursive Least Squares (RLS) algorithm is to update the weight vector by the least squares criterion in order to minimize the sum of squares of the array output error by adjusting the weight vector, which is different from the LMS algorithm, which minimizes the statistical average of the squared error. Its weight iteration formulation defined as below [10]:

$$\phi(n) = \lambda^{-1} \cdot P(n-1) \cdot x(n) \tag{42}$$

$$k(n) = \frac{\phi(n)}{1 + x^H(n) \cdot \phi(n)} \tag{43}$$

$$e(n) = d(n) - x^H(n) \cdot w(n-1) \tag{44}$$

$$w(n) = w(n-1) + k(n) \cdot e^*(n) \tag{45}$$

$$P(n) = \lambda^{-1} \cdot P(n-1) - \lambda^{-1} \cdot k(n) \cdot \phi^H(n) \tag{46}$$

Where $\mathbf{w}(n)$ and $\mathbf{w}(n-1)$ are the weight vectors at the current and previous time steps, respectively, $\mathbf{x}(n)$ is the the received signal vector , $d(n)$ is the desired signal, $e(n)$ is the estimation error, $\mathbf{P}$ are the inverses of the autocorrelation matrices, $\mathbf{k}(n)$ is the gain vector, $\phi(n)$ is an intermediate variable, λ is the forgetting factor, controlling the influence of past data.

C. Simulated Results

In our experiment, we simulate 250 snapshots with $\sigma_n^2 = 0.0001$. Appling LMS and RLS Beamformer with desired 90° DOA, the Array Pattern illustrated as Fig. 17 and Fig. 18.

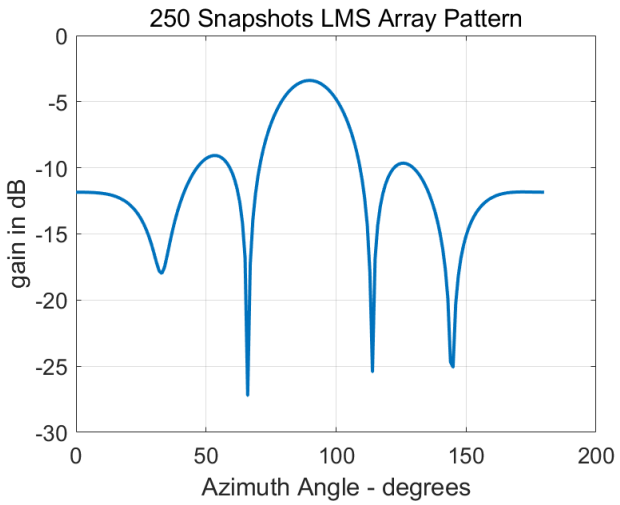

Fig. 17: The 250 Snatshots LMS Array Pattern(90^o)

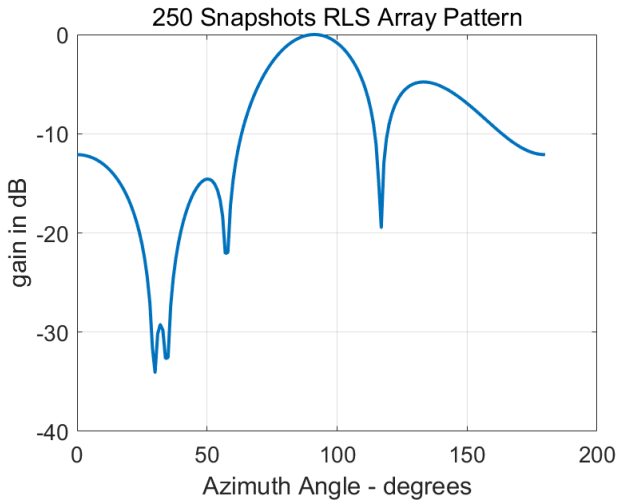

Fig. 18: The 250 Snatshots RLS Array Pattern(90^o)

We can find that the LMS Beamfomer fails to form nulls at the two unknown interference DOAs (30°, 35°). Nonetheless the RLS Beamfomer can perform well to suppress all interference DOAs. This also prove that the latter is more sophisticated and powerful than the former.

ACKNOWLEDGMENT

I am grateful to Professor A. Manikas for his insightful ideas greatly contributing to our laboratory design. I also wish to express my appreciation to Mr. Xinze Lyu for guiding me in conducting the experiments and answering my inquiries with clarity and patience. Their guidance and support have significantly enhanced my research and learning experience.

REFERENCES

[1] A. Manikas, "Differential geometry in array processing(2004)". Imperial College Press.
[2] A. Manikas, "AM Experiment Handout on Array Communication and Processing", October. 1998.
[3] A. Manikas, "Advanced communication theory lecture slides and notes" Sep. 2023. Available online: https://skynet.ee.ic.ac.uk/notes/notes.html
[4] T. Shan, M. Wax, T. Kailath, "On Spatial Smoothing for Direction-of-Arrival Estimation of Coherent Signals", IEEE Transactions on Acoustics, Speech and Signal Processing, Vol. ASSP-33, No.4, pp 806-811, August 1985.
[5] P. D. Karaminas and A. Manikas, "Super-resolution broad null beamforming for cochannel interference cancellation in mobile radio networks", IEEE Transactions on Vehicular Technology, Vol. 49, No. 3, pp. 689-697, May 2000
[6] A. Sleiman and A. Manikas, "Antenna array manifold: a simplified representation," 2000 IEEE International Conference on Acoustics, Speech, and Signal Processing. Proceedings (Cat. No.00CH37100), Istanbul, Turkey, 2000, pp. 3164-3167 vol.5, doi: 10.1109/ICASSP.2000.861209.
[7] A. Manikas, R. Karimi and 1. Dacos, "Study of the Detection and Resolution Capabilities of OneDimensional Array of Sensors by using Differential Geometry", IEE Proceedings on Radar, Sonar Navigation, vol. 141, No. 2, pp 83-92, April 1994.
[8] M. Wax and T. Kailath, "Detection of signals by information theoretic criteria", IEEE Transactions on Acoustics, Speech, and Signal Processing, Vol. 33, No. 2, pp. 387-392, April 1985.
[9] R. Schmidt, "Multiple Emitter Location and Signal Parameter Estimation", IEEE Transactions on Antennas and Propagation, Vol. AP-34, No.3, pp. 276-280, March 1986.
[10] S. Werner, "Reduced complexity adaptive filtering algorithms with applications to communications systems", Ph.D. dissertation, Helsinki University of Technology, Helsinki, Finland, Oct. 2002.
[11] B. D. Van Veen and K. M. Buckley, "Beamforming: a versatile approach to spatial filtering," in IEEE ASSP Magazine, vol. 5, no. 2, pp. 4-24, April 1988, doi: 10.1109/53.665.
[12] Aziz A, Qureshi M A, Iqbal M J, et al. Performance and quality analysis of adaptive beamforming algorithms (LMS, CMA, RLS & CGM) for smart antennas[C]//International Conference on Computer and Electrical Engineering. 2010, 6: 302-306.